Available online at www.sciencedirect.com
SCIENCE DIRECT
Biochimica et Biophysica Acta 1713 (2005) 65 – 72
BIOCHIMICA ET BIOPHYSICA ACTA
BBA
http://www.elsevier.com/locate/bba

Diffusion measurements of water, ubiquinone and lipid bilayer inside a cylindrical nanoporous support: A stimulated echo pulsed-field gradient MAS-NMR investigation

Olivier Wattraint*, Catherine Sarazin

Unité de Génie Enzymatique et Cellulaire, UMR 6022 du CNRS, Université de Picardie Jules Verne, 33 rue Saint-Leu, 80039 Amiens cedex, France

Received 21 March 2005; received in revised form 3 May 2005; accepted 4 May 2005
Available online 23 May 2005

Abstract

Stimulated echo pulsed-field gradient ^{1}H magic angle spinning NMR has been used to investigate the mobility of water, ubiquinone and tethered phospholipids, components of a biomimetic model membrane. The diffusion constant of water corresponds to an isotropic motion in a cylinder. When the lipid bilayer is obtained after the fusion of small unilamellar vesicles, the extracted value of lipid diffusion indicates unrestricted motion. The cylindrical arrangement of the lipids permits a simplification of data analysis since the normal bilayer is perpendicular to the gradient axis. This feature leads to a linear relation between the logarithm of the attenuation of the signal intensity and a factor depending on the gradient strength, for lipids covering the inner wall of aluminium oxide nanopores as well as for lipids adsorbed on a polymer sheet rolled into a cylinder. The effect of the bilayer formation on water diffusion has also been observed. The lateral diffusion coefficient of ubiquinone is in the same order of magnitude as the lipid lateral diffusion coefficient, in agreement with its localization within the bilayer.

Keywords: MAS-NMR PFG-STE; Tethered phospholipid bilayers; Nanoporous anodic aluminum oxide support; Oriented model membrane; Ubiquinone; Diffusion constants

1. Introduction

Customized biomimetic membranes are often used to study basic cellular function. Many reactions in membranes depend on the lateral motion and the fluid dynamic properties of all membrane components. The success of the development of model membranes involves the formation of a fluid single lipid bilayer allowing for a compartment mimicking the natural permeable barrier of the cell. Solid supported lipid membranes constitute a powerful approach to provide information on molecular processes occurring in biological membranes or some understanding of membrane–protein interactions as these models facilitate large transmembrane protein insertion [1–5]. These samples are highly suitable for biophysic studies due to their stability and robustness. One promising strategy consists of anchoring the lipid bilayer at one end to a spacer arm linked to a solid support [6,7].

Recently, a growing interest has emerged in a particular support: the anodic aluminium oxide support [8–14]. In the first report, the main interest in this support lies in the large surface area and a high volume concentration of membrane components as in naturally occurring membrane stacking in chloroplasts or mitochondria [8]. For the following reports, the interest was rather from an NMR

Abbreviations: AAO, anodic aluminum oxide; DOPE, 1,2-dioleoyl-sn glycero-3-phosphatidylethanolamine; EggPC, egg yolk L-α-phosphatidylcholine; HR-MAS, high resolution magic angle spinning; MLVs, multilamellar vesicles; NMR, nuclear magnetic resonance; PEG, polyethylene glycol; NHS, N-hydrosuccinimide; PET, polyethylene terephtalate; PFG-STE, pulsed-field gradient stimulated echo; POPC, 1-palmitoyl-2-oleoyl-sn-glycero-3-phosphatidylcholine; SUVs, small unilamellar vesicles

* Corresponding author. Tel.: +33 3 22 82 74 71; fax: +33 3 22 82 75 95.
E-mail address: Olivier.Wattraint@u-picardie.fr (O. Wattraint).

0005-2736/$ - see front matter © 2005 Elsevier B.V. All rights reserved.
doi:10.1016/j.bbamem.2005.05.005

spectroscopy point of view, namely alignment of the sample in the magnetic field to enhance spectral resolution [9–14]. Indeed, the lipid bilayer, with (or without) protein embedded, covers the inner cylindrical pore surface of this support commonly used as filters. This supported model membrane seems to be an alternative approach to the various model membranes for structural solid-state NMR spectroscopic studies of complex membrane proteins coated on glass plates or bicelles [15–17].

Solid-state NMR also provides a study of molecular motions covering a large range of dynamic processes occurring in biological membranes [18]. This technique seems to be well suited for a non-invasive study; indeed, it does not require a fluorophore probe nor a planar surface as in the case of Fluorescence Recovery After Photo bleaching. In some NMR approaches, lateral diffusion can be extracted from exchange spectroscopy [19] and with higher precision by using a spherical support [20]. Another type of experiment consists of using pulsed-field gradients combined with stimulated echo sequences [21]. A series of bipolar gradients can be used to produce higher effective gradient strengths [22]. In a recent approach [23], diffusion measurements have been obtained by the combination of pulsed-field gradient experiments with magic angle spinning which allow for high spectral resolution. Advantages of PFG-STE solid-state NMR has been demonstrated on magnetically aligned bicelles [24].

In this report, we propose to examine by ^{1}H PFG-STE NMR the diffusion of the components of a tethered model membrane inside AAO. The diffusion of water, lipids and ubiquinone, a small diffusive molecule, a key component in the electron transport chains of mitochondrial and bacterial membranes, has been achieved. We have observed the effect of the cylindrical orientation of the lipids and the effect of the lipid bilayer formation through fusion of small unilamellar vesicles.

2. Materials and methods

2.1. Sample preparation

The AAO Anodisc 47 discs (Whatman, Maidstone, England) with a pore diameter of 200 nm and a thickness of 60 μm have a porosity of 80% and a pore density of 2.54×10^{9} pores per cm^{2}. The Anodiscs were cut into discs of about 3 mm diameter in order to stack 120 fully hydrated discs into a 4 mm MAS rotor. Amino groups were linked to the AAO surface by reaction with (3-aminopropyl) dimethylethoxysilane (Aldrich, Strasbourg, France). Then, the discs were dipped for 45 min in a 2.1-mM NHS-biotin solution in a phosphate buffer. After extensive rinsing, the supports were dipped for 10 min in a 40-mg/ml streptavidin (Sigma, Saint Louis, MO, USA) solution in a PBS buffer (phosphate buffer 0.01 M and NaCl 0.15 M). The supports were rinsed with an octylglucoside solution and then with the PBS buffer before mixing for 1 h with SUV mixture. The SUVs, composed of egg yolk L-α phosphatidylcholine, egg-PC, (Sigma, Saint-Louis, MO, USA) and 1,2-dioleoyl-*sn*-glycero-3-phosphatidylethanolamine, DOPE (Sigma, Saint Louis, MO, USA), in a molar ratio of 64.5/35% and containing 0.5% of 1,2-dipalmitoyl-*sn*-glycero-3-phosphatidylethanolamine-N-biotinyl (Avanti Polar Lipids, Alabaster, AL, USA) were obtained by sonication of the mixture at a concentration of 5 mM. The size of the vesicles was in the range of 30–50 nm. Fusion was promoted by treatment with a 30% (w/v) polyethylene glycol, PEG_{8000}, (Sigma, Saint Louis, MO, USA) solution. After rinsing the PEG, the final Tris buffer (pH 7.5) was introduced. The experiments with ubiquinone Q_{10} (Sigma, Saint Louis, MO, USA) were obtained from SUVs as mentioned above in a ratio of 1:2 (mol/mol) ubiquinone and phospholipids. For NMR diffusion measurements, the final buffer was replaced by deuterated water (99.9%, Merck, Germany).

For adsorbed phospholipids on a polymer film, 10 mg of EggPC dissolved in chloroform were spread on a polyethylene terephtalate, PET, strip. Chloroform was evaporated under vacuum in a closed vessel and then hydration was obtained with deuterated water in a saturated atmosphere for 2 days at 55 °C.

Multilamellar Vesicles (MLVs) were obtained by mixing 20 mg of EggPC in 100 μl of deuterated water. A homogeneous multilamellar dispersion was obtained by 4 cycles of freeze–thawing.

2.2. NMR experiments

The experiments were performed on a Bruker 500 Avance spectrometer (Wissembourg, France) with an 11.7 T field. The spectra were acquired at a resonance frequency of 500.13 MHz with a 4.2-μs 90° pulse and a 5-s delay between scans. The spectral width was 5 kHz and the number of acquisitions was 256. The 4-mm PFG-MAS probe with *z*-axis gradients was operated at a spinning rate of 5 kHz.

^{1}H NMR diffusion measurements were conducted using a PFG-STE sequence with sine-shaped bipolar gradient pulses of 1 ms duration and a longitudinal eddy current delay of 5 ms. Diffusion times were varied from 50 ms to 1 s. For each diffusion time, 16 different values of gradient strength varying from 0.01 to 0.60 T/m were used. At every gradient strength, 256 scans were acquired with a recycle delay of 5 s. Spectra were processed with an exponential multiplication equivalent to 3 Hz line broadening before Fourier transformation and were referenced to HDO. All measurements were performed at 30 °C.

The gradient strengths were calibrated on residual water (HDO) using a 20-μl deuterated water filled HR-MAS rotor with a spherical insert. The diffusion coefficient obtained for HDO, $(1.60 \pm 0.15) \times 10^{-9}$ m^{2} s^{-1} at 22 °C, was comparative to the value given by Bruker (1.872×10^{-9} m^{2} s^{-1} at 25 °C). The accuracy of the resonance intensities was within 5%.

The standard deviation of the diffusion constants was obtained from the different values of apparent diffusion coefficients at steady-state.

3. Results

Fig. 1 illustrates the arrangement of the supported phospholipid bilayers tethered inside the inner pores of the AAO support. This solid support allowed for a cylindrical geometry of phospholipid bilayers inside the pores of 200 nm diameter and 60 μm length. The lipid bilayer, obtained by fusion of biotinylated SUVs, was tethered through a biotin/streptavidin spacer which was covalently linked to the support via an aminosilane bond. In this assembly of about 15 nm, the phospholipid bilayers mimicked the barrier between an internal compartment and an external compartment in which water and other molecules can diffuse. In a preliminary work, we had shown that the bound quantity of phospholipids was consistent with the covering of one bilayer per pore [12]. For NMR experiments, AAO discs were stacked in the rotor and this design had previously been used to assess the degree of alignment of the lipid bilayer inside the nanoporous support [14].

^{1}H NMR spectrum under 5 kHz MAS at 30 °C of the system is shown in Fig. 2. In these studies, the phospholipid bilayers were composed of 64.5% (mol/mol) of Egg-PC, 35% of DOPE and 0.5% of biotinylated DPPE. This mixture of low T_m ensures a fluid phase as shown by the well-resolved ^{1}H spectrum. The interesting resonance of lipid and ubiquinone are pointed out in Fig. 2, the assignment had been previously reported [12,25]. Ubiquinone was introduced into the lipid SUVs before fusion. In order to attenuate the water signal, the bathing buffer medium was replaced by D_2O.

The PFG NMR method which is well established in studies of molecular diffusion in isotropic liquids [26] has already been applied to examine lateral diffusion in lipid bilayers macroscopically aligned in a magnetic field. In liquid-state NMR experiments, samples were stacked between glass plates with the bilayer normal parallel to B_0 [27]. In recent works, static magic angle methods with a goniometer probe were applied to determine diffusion coefficients of membrane components sandwiched between oriented glass plates [28,29]. In HR-MAS probe, the gradient axis is collinear to the rotor axis, and thus in the model described in Fig. 3, the lipid membrane normal is then perpendicular to the gradient axis. For a random orientation of the membrane normal, the longitudinal ($D_{//}$) and transverse ($D_{\perp}$) diffusion coefficients must be considered. Due to the size of the AAO pores, for each cylinder, $D_{\perp}$ can be neglected leading to $D_{//}=D$ [30]. Thus, the equation of the normalized echo amplitude (R) over all solid angles given by Callaghan et al. [30] is:

$$R = e^{-kD}\int_0^1 e^{kDx^2}\mathrm{d}x \qquad (1)$$

where $x=\cos(\theta)$, θ is the angle between the bilayer normal and the axis of the field gradient. D is the diffusion constant, and k depends on: γ, the gyromagnetic ratio of protons; g, the gradient strength; δ, the gradient pulse length; Δ, the diffusion time between the two gradient pulses; T, the time between the gradient pulses, according to the equation:

$$k = 4\cdot\gamma^2 g^2 \delta^2\left(\Delta - \frac{T}{2} - \frac{\delta}{8}\right) \qquad [31]$$

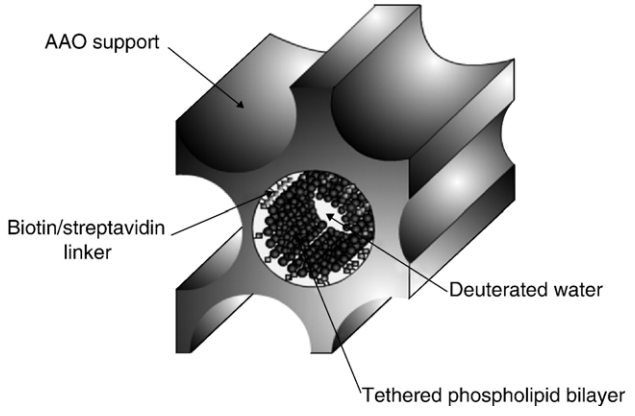

Fig. 1. Illustration of a phospholipid bilayer tethered inside a nanopore of AAO.

3.1. Water diffusion and porosity

In our biomimetic model, the diffusional motion of water occurred randomly inside the cylinders. The attenuation of NMR signal intensity, after application of two gradient pulses separated by a diffusion time, Δ, was given by Eq. (1).

According to Gaede and Gawrisch [31], rewriting the echo attenuation (R) as $\ln(I/I_0)$, Eq. (1) can be approximated by:

$$\ln\left(\frac{I}{I_0}\right) = -\frac{2}{3}kD + \frac{2}{45}(kD)^2 \qquad (2)$$

This Eq. (2) was used to fit the data obtained for the HDO resonance in the nanoporous support with and without tethered lipid bilayers (Fig. 4). For each diffusion time (Δ), an apparent diffusion coefficient (D_{app}) was extracted. From a plot of D_{app} as a function of diffusion times, Δ, at 30 °C, the water diffusion coefficient (D) was equal to 1.1×10^{-9} m^2 s^{-1} and 1.0×10^{-9} m^2 s^{-1} without lipids and in presence of the tethered lipid bilayers, respectively. There is no significant difference between these two values indicating a good diffusion of water along the nanopores. This study has been undertaken before the fusion of SUVs leading to a water diffusion coefficient of 4.7×10^{-10} m^2 s^{-1}, this effect will be discussed later.

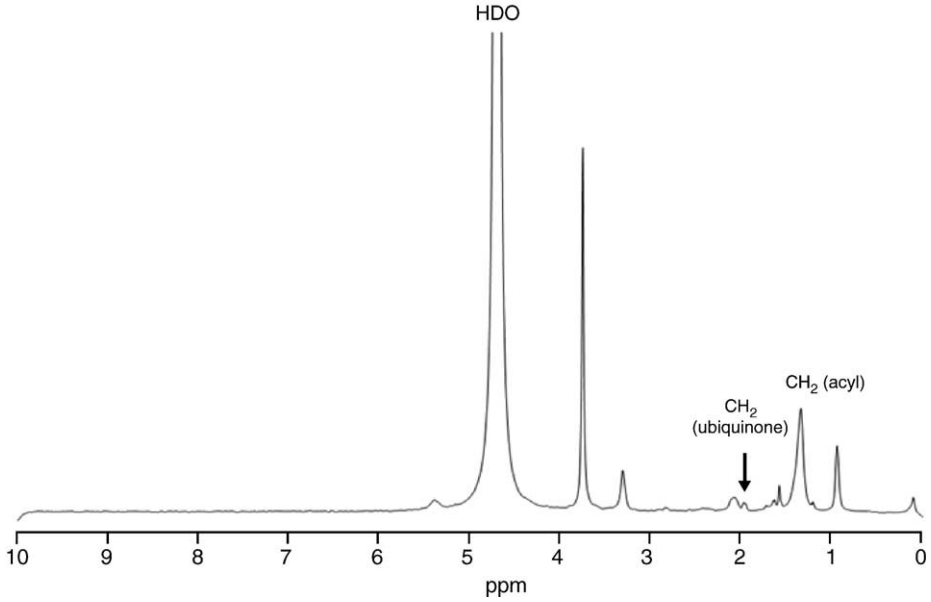

Fig. 2. ^{1}H MAS (5 kHz) NMR spectrum of tethered phospholipid bilayers and ubiquinone 2:1 (mol/mol) inside AAO.

The effect of the cylindrical restriction on water diffusion has been approximated by Gibbs [32] by the following equation:

$$\frac{D_{\mathrm{app}}}{D_0} = \left[1 + \frac{4}{3\sqrt{\pi}}\sqrt{D_0\frac{\Delta}{r^2}} - 1.81\left(D_0\frac{\Delta}{r^2}\right)^{0.81} + 4\left(D_0\frac{\Delta}{r^2}\right)\right]^{-1} \quad (3)$$

where r is the radius of the cylinder and D_0 is the diffusion constant of bulk water.

This approximation has already been applied on muscle fibers [33]. Indeed, the use of giant fibers in their study minimizes the effect of restriction within the cylindrical sarcolemma, allowing an examination of intracellular barriers. We considered that the fraction of water restricted inside the AAO cylindrical pores, which diffused according to the Eq. (3), can be assimilated to the porosity. In Fig. 5, the best agreement between the experimental data and simulation is shown. At short diffusion times, there was no cylindrical restriction on water diffusion. At long diffusion times, above 250 ms, this constraint was visible. In order to take into account the fraction of unrestricted water, we considered a linear behaviour between the normalized D_{app} and Δ. The simulation of experimental data in Fig. 5 is then obtained by adding a fraction of restricted water and the complementary fraction of unrestricted water. The porosity corresponded to the contribution of the restricted water. In the case of the naked aluminium oxide support filled with deuterated water, the radius was equal to 200 nm and the best fit was obtained for a porosity of 78% through Eq. (3), corresponding to the water diffusion inside the nanopores. This value was in good agreement with the porosity given by the manufacturer (80%). When lipid bilayers were tethered inside the pores, the radius of the inner pore was decreased by about 15 nm considering first the biotinylation of the support (2.3 nm), the streptavidin spacer (5 nm), the biotinylated lipids (2.3 nm) and finally the lipid bilayer (5 nm) [34]. In this case, a porosity of 84% resulted from the best fit with Eq. (4). This result was in agreement with the previous result on the naked support since the porosity did not change but validated the hypothesis of the diameter decrease when the lipid bilayer covers the inner pore surface. Furthermore, in the stacked discs of the tethered sample, most of the water diffused through the pores, meaning that the diffusion of water in the bathing medium represented less than 20%.

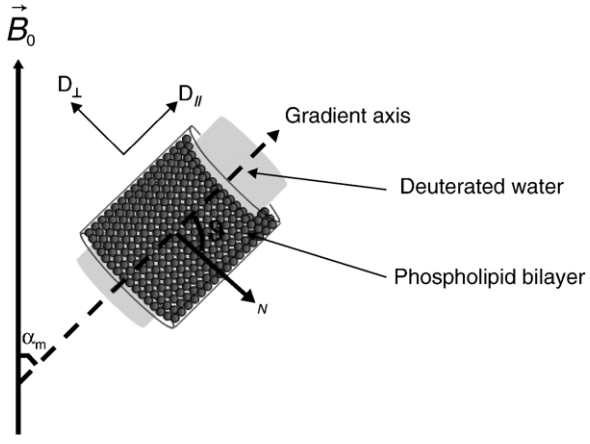

Fig. 3. Schematic representation of phospholipids and water inside a nanopore. The gradient axis defines the direction of the pore. The bilayer normal is given by N. θ is the angle between the gradient axis and N. $D_{//}$ and $D_{\perp}$ are respectively, the longitudinal and the transverse component of the measured diffusion constant.

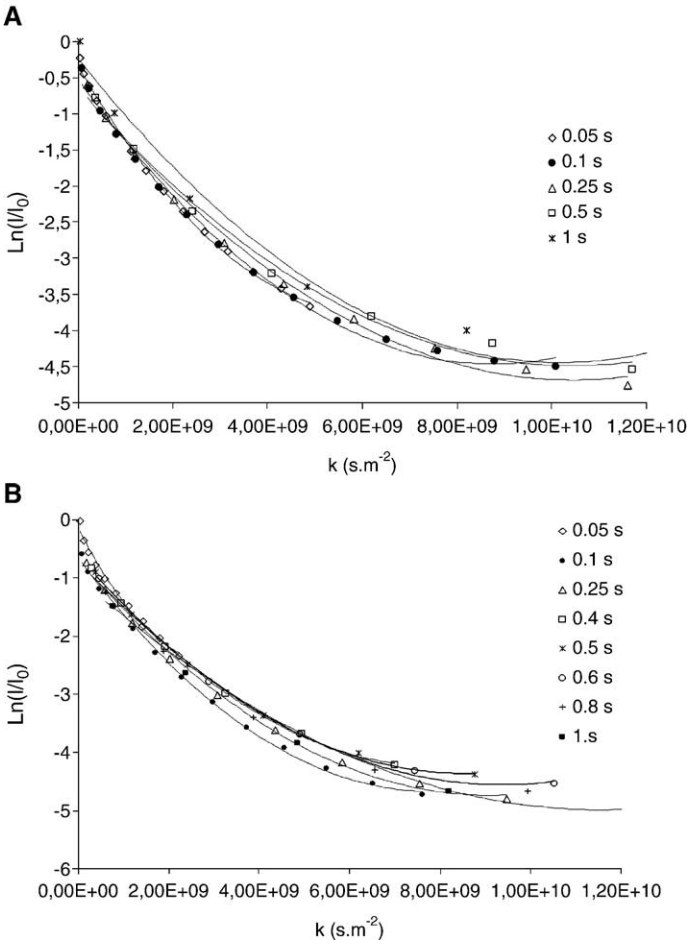

Fig. 4. Plot of the normalized ln of the attenuation of the intensity of HDO resonance vs. k for different diffusion times (A) for deuterated water in the naked AAO support and (B) for deuterated water in the tethered phospholipid bilayers inside the AAO support.

3.2. Lipid diffusion

When the discs were stacked in the rotor set at the magic angle, the normal of the lipid bilayers tethered inside the nanopores was perpendicular to the rotor axis and thus, to the axis of the field gradient (Fig. 3). For this orientation, Eq. (1) can be simplified since $\cos(\theta)$ is null. The attenuation of the normalized signal intensity is now given by the following equation:

$$\frac{I}{I_0} = e^{-kD} \tag{4}$$

In order to verify this hypothesis without ambiguity, we chose to use a simplified sample allowing for a higher quantity of lipids (about 10 mg) than in the AAO sample (about 2 mg). In this simplified sample, a phospholipid film of the same composition was adsorbed on a polymer sheet (PET) rolled into a cylinder. This sample preserved the distribution of the bilayer normal orientation [14,35]. Only one diffusion time was reported here since our goal was not to obtain a precise value of the diffusion constant but to verify the linear relationship as derived from Eq. (4). For a diffusion time of 250 ms, the plot of the logarithm of the integrated signal of the methylene resonance of phospholipid acyl groups versus k is reported in Fig. 6. This graph shows evidence of the linearity of the relationship between ln I/I_0 and k, leading to an apparent diffusion coefficient (D_{app}) value of 4.7×10^{-12} m^2 s^{-1} with a correlation coefficient of 0.966.

To study the diffusion of lipids tethered inside the AAO, a plot of the logarithm of the integrated signal of the methylene resonance of phospholipid acyl (1.3 ppm) groups versus k is reported in Fig. 7A. For each diffusion time, the experimental data could be fitted linearly as in the case of the adsorbed sample on PET. The scattering of the experimental data was a consequence of the low lipid concentration. The corresponding slope gave the apparent diffusion coefficient. The obtained D_{app} were plotted as a function of Δ (Fig. 7B). A steady-state value of $(1.7\pm0.2)\times10^{-12}$ m^2 s^{-1} was reached for the lateral diffusion coefficient (D) after a diffusion time of 250 ms. This value agreed with the lateral diffusion coefficient of phospholipids $(2.8\pm0.4)\times10^{-12}$ m^2 s^{-1} obtained by ^{31}P NMR spin–spin relaxation time with a spherical geometry [12]. This observation emphasises the benefit of

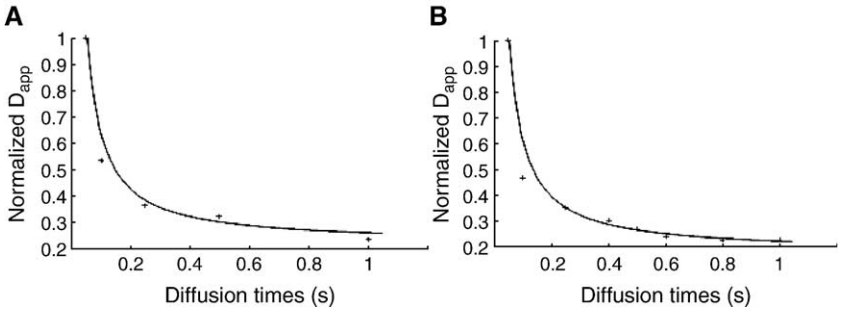

Fig. 5. Plot of normalized D_{app} as a function of diffusion times. (A) For deuterated water in the naked AAO support and (B) for deuterated water in the tethered phospholipid bilayers inside the AAO support.

the orientation of the normal bilayer to determine the diffusion coefficient on a cylinder. Considering the lipid diffusion on a cylindrical surface, the steady-state observed for rather long diffusion time suggests that the domain size is at least 8 micrometers in the range of diffusion times that can be explored before decay to undetectable values.

The effect of the bilayer formation was investigated by measuring the diffusion coefficient on the sample after the loading of SUVs at only two diffusion times in order to avoid the spontaneous fusion process. The obtained value was $(1.7 \pm 0.1). \times 10^{-12}$ m^2 s^{-1}.

3.3. Diffusion of ubiquinone in the tethered lipid bilayer

Ubiquinone Q_{10} is an antioxidant molecule comprising of a polar head group and a long tail of ten isoprenyl units. The interesting signal of ubiquinone for the diffusion measurement is the methylene resonance of the decaprenyl part at 1.96 ppm (Fig. 2).

The lateral diffusion coefficient of Q_{10} in the tethered lipid bilayer environment was obtained from the measurements of the signal attenuation and was fitted either with Eq. (2) or Eq. (4). In both cases, the values obtained were coherent and convergent towards an average value of 2.1×10^{-12} m^2 s^{-1}.

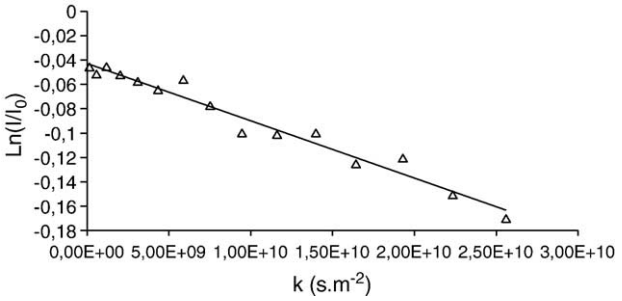

Fig. 6. Plot of the normalized ln of the attenuation of the intensity of the methylene acyl group resonance vs. k for different diffusion times for phospholipid bilayers adsorbed on a polymer sheet.

4. Discussion

Table 1 sums up the diffusion constants of water, lipid and ubiquinone in the tethered model membrane inside the cylindrical pores of AAO. In order to refer to other values obtained by PFG-STE measurements on a classical model, the values obtained for the same composition on MLVs are reported. These last values were obtained by the polynomial fit with Eq. (2).

Before the fusion of SUVs inside the nanopores, the observed value for water was in the same order of magnitude as in MLVs. Depending on the hydration state

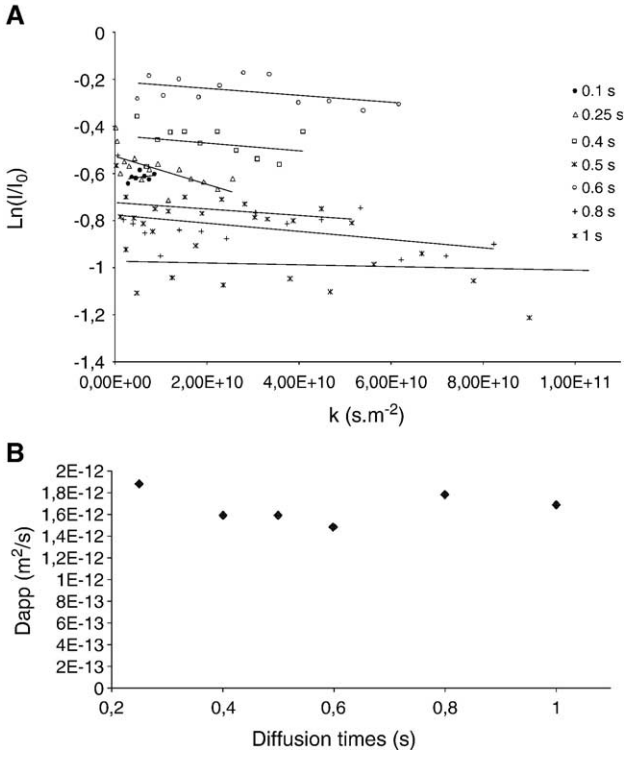

Fig. 7. (A) Plot of the normalized ln of the attenuation of the intensity of the methylene acyl group resonance vs. k for different diffusion times and (B) plot of D_{app} as a function of diffusion times for phospholipid bilayers tethered inside the AAO support.

Table 1
Diffusion constants of water, lipids and ubiquinone in different biomimetic models determined by PFG-STE

D (m^2 s^{-1}) at 303 K	MLVs	AAO	
		Before fusion	After fusion
Water (HDO)	$(0.9\pm0.2)\times10^{-10}$	$(4.7\pm0.1)\times10^{-10}$	$(1.0\pm0.1)\times10^{-9}$
Lipids	$(3.7\pm0.1)\times10^{-12}$	$(1.7\pm0.1)\times10^{-12}$	$(1.7\pm0.2)\times10^{-12}$
Ubiquinone Q_{10}	$(1.7\pm0.1)\times10^{-12}$	–	$(1.8\pm0.2)\times10^{-12}$

of the MLVs, for lower hydration, the diffusion constant can reach 3×10^{-10} m^2 s^{-1} at 296 K [31]. The AAO model allowed for a higher hydration state. The drastic effect of the fusion was observed on the water diffusion constant: a value two times greater was obtained after the formation of the lipid bilayer. These results clearly indicate that the formation of the lipid bilayer was promoted by the fusion of SUVs. The water diffusion observed after fusion was close to the free water diffusion in the naked AAO support, showing that there was no obstruction due to unfused SUVs. The fusion had no significant effect on lipid diffusion and these values ranged in those expected for a biomimetic phospholipid membrane: from 1 to 10×10^{-12} m^2 s^{-1} [28]. The diffusion coefficients can be affected by the nature of the phospholipids and also by the experiment temperature. Since the majority of the SUVs were anchored to the streptavidin sublayer, the D value obtained before the fusion was similar to that after fusion. This hypothesis indicated restricted rotational diffusion of the SUVs. In the case of an adsorbed bilayer of POPC inside the AAO nanotubes, a D value of 4.6×10^{-13} m^2 s^{-1} was reported indicating that diffusion distances were restricted by the size of lipid patches [10]. However, in the case of the tethered model reported in this work, this limitation did not seem to take place considering the D value (Table 1). Indeed, the incorporation of phosphatidylethanolamine in the SUV mixture improves the fusion confirming the role of lipids in the fusion process to obtain a single fluid lipid bilayer [36,37].

For the phospholipid mixture adsorbed on the polymer sheet, a previous work had shown a bilayer alignment of 75% with a mosaic spread of 8° [12]. The remaining non-oriented lipids could contribute to a lack of precision in the lipid diffusion constant. Although the alignment in the AAO model is higher (89%) [14], the limitation in the determination of the lateral diffusion coefficient was due to the low quantity of both lipids and ubiquinone. The diffusion value of ubiquinone in the tethered lipid model as reported in Table 1 was the result of the linear fit. This value, ranging in the lipid diffusion value, suggested that ubiquinone was embedded in the lipid bilayer and presented a lateral diffusion along the bilayer plane due to its hydrophobic tail without more precise information on its insertion [25]. The diffusion of Q_{10} was in good agreement with electrochemical measurements [8]. PFG-STE experiments gave a good estimation of diffusion measurements in a simple manner for supported membranes in porous systems.

Acknowledgement

The authors thank Trixie Ann Bartholomeusz for linguistic advice.

References

[1] B. Raguse, V. Braach-Maksvytis, B.A. Cornell, L.G. King, P.D.J. Osman, R.J. Pace, L. Wieczorek, Tethered lipid bilayer membranes: formation and ionic reservoir characterisation, Langmuir 14 (1998) 648–659.
[2] R. Naumann, E.K. Schmidt, A. Jonczyk, K. Fendler, B. Kadenbach, T. Liebermann, A. Offenhaüsser, W. Knoll, The peptide-tethered lipid membrane as a biomimetic system to incorporate cytochrome *c* oxidase in a functionally active form, Biosens. Bioelectron. 14 (1999) 651–662.
[3] S.G. Boxer, Molecular transport and organization in supported lipid membranes, Curr. Opin. Chem. Biol. 4 (2000) 704–709.
[4] E.S. Sinner, W. Knoll, Functional tethered membranes, Curr. Opin. Chem. Biol. 5 (2001) 705–711.
[5] M.O. Jensen, O.G. Mouritsen, Lipids do influence protein function—The hydrophobic matching hypothesis revisited, Biochim. Biophys. Acta 1666 (2004) 205–226.
[6] E. Sackmann, M. Tanaka, Supported membranes on soft polymer cushions: fabrication, characterization and applications, Trends Biotechnol. 18 (2000) 58–64.
[7] R.P. Richter, J. Lai Kee Him, A. Brisson, Supported lipid membranes, Materials Today 6 (2003) 32–37.
[8] V. Proux-Delrouyre, J.M. Laval, C. Bourdillon, Formation of streptavidin-supported lipid bilayers on porous anodic alumina: electrochemical monitoring of triggered vesicle fusion, J. Am. Chem. Soc. 123 (2001) 9176–9177.
[9] A.I. Smirnov, O.G. Poluektov, Substrate-supported lipid nanotube arrays, J. Am. Chem. Soc. 125 (2003) 8434–8435.
[10] H.C. Gaede, K.M. Luckett, I.V. Polozov, K. Gawrisch, Multinuclear NMR studies of single lipid bilayers supported in cylindrical aluminum oxide nanopores, Langmuir 20 (2004) 7711–7719.
[11] G.A. Lorigan, P.C. Dave, E.K. Tiburu, K. Damodaran, S. Abu-Baker, E.S. Karp, W.J. Gibbons, R.E. Minto, Solid-state NMR spectroscopic studies of an integral membrane protein inserted into aligned phospholipids bilayer nanotube arrays, J. Am. Chem. Soc. 126 (2004) 9504–9505.
[12] O. Wattraint, A. Arnold, M. Auger, C. Bourdillon, C. Sarazin, Lipid bilayer tethered inside a nanoporous support: a solid-state nuclear magnetic resonance investigation, Anal. Biochem. 336 (2005) 253–261.
[13] E.Y. Chekmenev, J. Hun, P.L. Gor'kov, W.W. Brey, T.A. Cross, A. Ruuge, A.I. Smirnov, 15N and 31P solid-state NMR study of transmembrane domain alignment of M2 protein of influenza A virus in hydrated cylindrical lipid bilayers confined to anodic aluminum oxide nanopores, J. Magn. Reson. 173 (2005) 322–327.
[14] O. Wattraint, D.E. Warschawski, C. Sarazin, Tethered or adsorbed supported lipid bilayers in nanotubes characterized by deuterium magic angle spinning NMR spectroscopy, Langmuir 21 (2005) 3226–3228.
[15] G. Gröbner, A. Taylor, P.T.F. Williamson, G. Choi, C. Glaubitz, J.A. Watts, W.J. de Grip, A. Watts, Macroscopic orientation of natural and

model membranes for structural studies, Anal. Biochem. 254 (1997) 132–138.
[16] C.R. Sanders, K. Oxenoid, Customizing model membranes and samples for NMR spectroscopic studies of complex membrane proteins, Biochim. Biophys. Acta 1508 (2000) 129–145.
[17] I. Marcotte, M. Auger, Bicelles as model membranes for solid- and solution-state NMR studies of membrane peptides and proteins, Concepts Magn. Reson. 24A (2005) 17–37.
[18] A. Watts, Solid-state NMR approaches for studying the interaction of peptides and proteins with membranes, Biochim. Biophys. Acta 1376 (1998) 297–318.
[19] D.B. Fenske, H.C. Jarrell, Phosphorus-31 two-dimensional solid-state exchange NMR. Application to model membrane and biological systems, Biophys. J. 59 (1991) 55–69.
[20] F.M. Picard, M.-J. Paquet, E.J. Dufourc, M. Auger, Measurement of the lateral diffusion of dipalmitoylphosphatidylcholine adsorbed on silica beads in the absence of melitin: a ^{31}P two-dimensional exchange solid-state NMR study, Biophys. J. 83 (1998) 857–868.
[21] J.E. Tanner, Use of the stimulated echo in NMR diffusion studies, J. Chem. Phys. 52 (1970) 2523–2526.
[22] D. Wu, A. Chen, C.S. Johnson, An improved diffusion-ordered spectroscopy experiment incorporating bipolar-gradient pulses, J. Magn. Reson. 115 (1995) 260–264.
[23] A. Pampel, D. Michel, R. Reszka, Pulsed field gradient MAS-NMR studies of the mobility of carboplatin in cubic liquid-crystalline phases, Chem. Phys. Lett. 357 (2002) 131–136.
[24] R. Soong, P.M. Macdonald, Lateral diffusion of PEG-lipid in magnetically aligned bicelles measured using stimulated echo pulsed field gradient 1H NMR, Biophys. J. 88 (2005) 255–268.
[25] M. Afri, B. Ehrenberg, Y. Talmon, J. Schmidt, Y. Cohen, A.A. Frimer, Active oxygen chemistry within the liposomal bilayer: Part III. locating vitamin E, ubiquinol and ubiquinone and their derivatives in the lipid bilayer, Chem. Phys. Lipids 131 (2004) 107–121.
[26] W.S. Price, Pulsed field gradient nuclear magnetic resonance as a tool for studying translational diffusion: part one. Basic theory, Concept. Magn. Reson. Imag. 9 (1997) 299–336.
[27] P. Karakatsanis, T.M. Bayerl, Diffusion measurements in oriented phopholipid bilayers by 1H NMR in a static fringe fid gradient, Phys. Rev., E 54 (1996) 1785–1790.
[28] A. Filippov, G. Orädd, G. Lindblom, The effect of cholesterol on the lateral diffusion of phospholipids in oriented bilayers, Biophys. J. 84 (2003) 3079–3086.
[29] G. Orädd, G. Lindblom, P.W. Westerman, Lateral diffusion of cholesterol and dimyristoylphosphatidylcholine in a lipid bilayer measured by pulsed field gradient NMR spectroscopy, Biophys. J. 83 (2002) 2702–2704.
[30] P.T. Callaghan, K.W. Jolley, J. Lelievre, Diffusion of water in the endosperm tissue of wheat grains as studied by pulsed field gradient nuclear magnetic resonance, Biophys. J. 28 (1979) 133–142.
[31] H.C. Gaede, K. Garwrisch, Lateral diffusion rates of lipid, water, and a hydrophobic drug in a multilamellar liposome, Biophys. J. 85 (2003) 1734–1740.
[32] S.J. Gibbs, Observations of diffusive diffraction in a cylindrical pore by PFG NMR, J. Magn. Reson. 124 (1997) 223–236.
[33] S.T. Kinsey, T.S. Moerland, Metabolite diffusion in giant muscle fibers of the spiny lobster *Panulirus argus*, J. Exp. Biol. 205 (2002) 3377–3386.
[34] V. Proux-Delrouyre, C. Elie, J.M. Laval, J. Moiroux, C. Bourdillon, Formation of tethered and streptavidin-supported lipid bilayers on a microporous electrode for the reconstitution of membranes of large surface area, Langmuir 18 (2002) 3263–3272.
[35] C. Sizun, B. Bechinger, Bilayer sample for fast or slow magic angle oriented sample spinning solid-state NMR spectroscopy, J. Am. Chem. Soc. 124 (2002) 1146–1147.
[36] P.R. Cullis, B. de Kruijff, The polymorphic phase behaviour of phosphatidylethanolamines of natural and synthetic origin: a 31P NMR study, Biochim. Biophys. Acta 513 (1978) 31–42.
[37] F. Deeba, H. Nasti Tahseen, K. Sharma Sharad, N. Ahmad, S. Akhtar, M. Saleemuddin, O. Mohammad, Phospholipid diversity: correlation with membrane-membrane fusion events, Biochim. Biophys. Acta 1669 (2005) 170–181.